Forces and extensions in semiflexible and rigid polymer chains and filaments

2007 J. Phys. A: Math. Theor. 40 10951

(http://iopscience.iop.org/1751-8121/40/36/001)

IOP PUBLISHING JOURNAL OF PHYSICS A: MATHEMATICAL AND THEORETICAL

J. Phys. A: Math. Theor. **40** (2007) 10951–10964 doi:10.1088/1751-8113/40/36/001

Forces and extensions in semiflexible and rigid polymer chains and filaments

J R Blundell and E M Terentjev

Cavendish Laboratory, University of Cambridge, J J Thomson Avenue, Cambridge, CB3 0HE, UK

E-mail: emt1000@cam.ac.uk

Received 5 May 2007, in final form 24 July 2007
Published 21 August 2007
Online at stacks.iop.org/JPhysA/40/10951

Abstract

We present a revised theoretical study of statistical properties of semiflexible filaments. Using a single auxiliary field and mean-field theory, we succeed in obtaining the exact analytical results for force–extension relations for a chain with arbitrary stiffness, and compare it with earlier theories and experiment. At a small persistence-to-contour length ratio, $l_p/L \ll 1$ the chain behaves classically, as an entropic spring. However, we find a critical value for $L/l_p \approx 3.0$ in 3D (or $L/l_p \approx 5.4$ in 2D) above which the restoring force of the chain becomes negative for the end-to-end distance $R_{3D}/L < \sqrt{1 - L/3l_p}$ (or $R_{2D}/L < \sqrt{1 - L/5.4l_p}$). That is, very stiff (or very short) chains and filaments resist an attempt to reduce their preferred end-to-end distance as much as to stretch it.

PACS numbers: 36.20.−r, 82.35.Lr, 87.15.−v

1. Introduction

The statistical properties of random-trajectory continuous chain models (the so-called Kratky–Porod or worm-like chain) have been the subject of intense study since they were introduced back in 1949 [1]. Since then there have been a number of successful models of polymer chains based on the 'mesoscopic' Hamiltonian—one neglecting the chemical details of the individual atoms in favour of a simplified worm-like space-curve. The semi-flexible worm-like chain is used to model polymers or filaments that possess an inherent stiffness, and is controlled by a single parameter: the bending energy in the Hamiltonian. Interest in the semi-flexible chain is understandable as there are many real macromolecules and assemblies that exhibit large chain stiffness, and as a consequence do not behave as Gaussian chains. Notable examples of such chains occur in biological systems such as DNA, actin filaments, fibrils, microtubules and in some liquid crystalline polymers. Modelling such chains therefore has a very real relevance.

There have been several successful recent studies of semi-flexible chains [2–5], which in turn refer back to numerous earlier efforts. However, few of these studies provide closed analytic expressions for the free energy of a single chain for all stiffnesses. One of the most successful techniques to study semi-flexible chains has been the functional integral method which employs mean-field theory [2, 3, 6]. Using mean-field theory simplifies the problem considerably; however, there are still serious difficulties in making the model analytically tractable. These stem mainly from the implementation of the constraints for the inextensibility of the chain.

In this paper, we return to this classical problem, calculating the properties of a single polymer chain, or semi-flexible filament, in mean-field theory. We use a single auxiliary mean field to implement a global constraint on the inextensibility of the chain. The model is presented in a much abbreviated form since there are important and substantial contributions already present in the literature. We concentrate on more delicate issues of developing the basic model, such as various constraints, the need of introducing additional Lagrange multiplier to deal with the ends of the chain [3] (which we shall assert is not needed) and the regime of rigid chains when the persistence length l_p is comparable or larger that the contour length L. Using a single auxiliary field, we succeed in evaluating the partition function for a single filament analytically, as a function of chain parameters and the constrained end-to-end distance R, which enables us to study radial distribution functions for chains of various stiffness. This is the central result of our work. We are then able to examine the behaviour of chains in both the semi-flexible and rigid regimes and compare them to experiment. Specifically we compare the experimental results on force–extension and end-to-end distribution functions for DNA molecules [7, 8] with the theoretical predictions of this new model.

We should highlight the important issue of self-avoidance. In the theory presented here, the chain self-avoidance has not been taken into account. Of course the real chains and filaments cannot cross themselves; however, the effect of self-avoidance (which is a famous and difficult problem on its own [9, 10]) is not expected to be relevant in the stiff-chain limit. The issue of self-avoidance will be important when we compare our model to force–extension data [7]. In these experiments the DNA chains studied are long enough that, at small extensions, they are certainly in the self-avoiding regime. It has been shown [11–13] that self-avoidance can have an important effect on the stretching response of polymer chains, so we must be careful not to read too much into comparisons between experimental stretching response at low extensions for long chains, and our model, as in these conditions self-avoidance will be an issue. Our main point, and interest, are in the opposite regime: of chains and filaments short enough or stiff enough to be nearly fully extended.

2. Model—mean field theory

2.1. Chains with constant extension: $\boldsymbol{r}$-space formalism

We begin by considering the discrete model for a stiff chain in d dimensions. In such a model, each of the N 'monomers' on the chain has position vector $\boldsymbol{r}_n$ while the 'bonds' are inextensible so that $\boldsymbol{r}_{n+1} - \boldsymbol{r}_n = b$. The stiff, or semi-flexible chain has an intrinsic bending rigidity. That is to say that it has an energy penalty associated with the bending away from the zero-temperature ground state, here taken to be a straight line (see [5] for the analysis of spontaneous curvature). The chain Hamiltonian therefore must incorporate a quadratic bending energy of the form $E_{\text{bend}} = \frac{1}{2}\kappa(r_{n+1} - 2r_n + r_{n-1})^2$. The partition function for such a

chain is therefore,

$$Z = \int \prod_{n=1}^{N-1} \frac{\mathrm{d}^d r_n}{L^d} \exp\left(-\beta \sum_{n=1}^{N-1} \frac{1}{2}\kappa(\boldsymbol{r}_{n+1} - 2\boldsymbol{r}_n + \boldsymbol{r}_{n-1})^2\right) \prod_{n=1}^{N-1} \delta[(\boldsymbol{r}_{n+1} - \boldsymbol{r}_n)^2 - b^2], \tag{1}$$

where $\beta = 1/k_\mathrm{B}T$ and the delta functions ensure the bond inextensibility constraint. As N becomes large, to a good approximation we can write

$$\boldsymbol{r}_{n+1} - 2\boldsymbol{r}_n + \boldsymbol{r}_{n-1} = b^2 \left(\frac{\partial^2 \boldsymbol{r}}{\partial n^2}\right)_{r=r_n} \qquad \boldsymbol{r}_{n+1} - \boldsymbol{r}_n = b\left(\frac{\partial \boldsymbol{r}}{\partial n}\right)_{r=r_n}. \tag{2}$$

Inserting these expressions and exponentiating the delta-functions in terms of the auxiliary field ϕ we obtain

$$Z = \int \prod_{n=1}^{N-1} \frac{\mathrm{d}^d r_n}{L}\, \mathrm{d}\phi_n \exp\left[b \sum_{n=1}^{N-1} \left[-\frac{l_p}{2}\ddot{\boldsymbol{r}}_n^2 + \mathrm{i}\phi_n\left(\dot{\boldsymbol{r}}_n^2 - 1\right)\right]\right], \tag{3}$$

where $\ddot{\boldsymbol{r}}$ and $\dot{\boldsymbol{r}}$ represent the second and first derivatives and the bending modulus κ is expressed through the parameter $l_p = \kappa b^3/k_\mathrm{B}T$. This length scale is directly related to the persistence length λ of the chain in d-dimensions of space, via $l_p = \lambda(d-1)/2$ see [2]. Note that we do not introduce an additional Lagrange multiplier to control the ends of the chain, which Ha and Thirumalai [3] and Winkler [6] suggest, is necessary. We will explicitly demonstrate that exactly the same expression for the partition function in the flexible limit is obtained with and without these additional constraints. Taking the limit that $N \to \infty$ and $b \to 0$ while keeping $Nb = L$ we transform the partition function to the path integral form

$$Z = \int \mathcal{D}\phi \mathcal{D}r(s) \exp\left[\int_0^L \mathrm{d}s \left(-\frac{l_p}{2}\ddot{\boldsymbol{r}}(s)^2 + \mathrm{i}\phi(s)[\dot{\boldsymbol{r}}(s)^2 - 1]\right)\right], \tag{4}$$

using the continuum variable for the arc length s in place of the discrete index $n \in (1, N)$, and the notation that $\mathcal{D}r(s) = \lim_{N\to\infty} \prod_{n=1}^{N-1} \frac{1}{L^d}\,\mathrm{d}^d r_n$ and $\mathcal{D}\phi(s) = \lim_{N\to\infty} \prod_{n=1}^{N-1} L\,\mathrm{d}\phi_n$. In this limit therefore, we regard the worm-like chain as a differentiable space-curve defined at every position by the vector $\boldsymbol{r}(s)$.

It is common to make the problem more analytically tractable by replacing the auxiliary field $\phi(s)$ with a mean value ϕ which is constant over the length of the chain (though will take a *different* value for each chain configuration). This is a significant approximation as the mean-field approach is equivalent to requiring that $\langle \dot{\boldsymbol{r}}^2 \rangle = 1$. That is, we replace the local constraint that $\dot{\mathbf{r}}^2 = 1$ everywhere along the curve with a single global condition of chain inextensibility. This transforms the integral into standard Gaussian form.

As with all path integral problems of this kind, the key to evaluating the resulting Gaussian integrals is in the boundary conditions. For any open trajectory in $\boldsymbol{r}$-space, the ends of the chain are separated by some end-to-end vector $\boldsymbol{R}$. We stress that since we are interested in the statistics of a single chain, it is this separation vector $\boldsymbol{R}$ that is the relevant variable in the problem and not the actual values of $\boldsymbol{r}(s)$. That is to say, when dealing with a single chain, configurations related by a translation are equivalent. For all regimes in the mean-field approach (both constant force and constant extension), the only boundary conditions on the chain therefore are that $\boldsymbol{r}(0) = \mathbf{0}$ and $\boldsymbol{r}(L) = \boldsymbol{R}$. These boundary conditions can be made homogeneous by the addition of a linear term

$$\boldsymbol{r}(s) = \frac{s}{L}\boldsymbol{R} + \boldsymbol{x}(s), \tag{5}$$

with $\boldsymbol{x}(0) = 0$ and $\boldsymbol{x}(L) = 0$. This is the problem of a ring polymer [14], and can be solved by employing the Fourier series:

$$\boldsymbol{r}(s) = \frac{s}{L}\boldsymbol{R} + \sum_{q=1}^{\infty} \boldsymbol{x}_q \sin\left(\frac{q\pi s}{L}\right). \tag{6}$$

This Fourier expansion clearly obeys the boundary conditions. It is similar to the standard Rouse expansion [15], in which a cosine is used in order to respect the force-free boundary condition typically found in a polymer melt.

The Fourier expansion transforms the partition function into an infinite series of decoupled Gaussian integrals

$$Z = L\int_{-\infty}^{\infty} \mathrm{d}\phi\, \mathrm{e}^{-\mathrm{i}\phi L(1-\rho^2)} \int \mathcal{D}\boldsymbol{x}_q \exp\left[-\frac{1}{2}\sum_{q=1}^{\infty} \boldsymbol{x}_q \cdot \boldsymbol{A}_q \cdot \boldsymbol{x}_q\right]$$
$$= L\int_{-\infty}^{\infty} \mathrm{d}\phi\, \mathrm{e}^{-\mathrm{i}\phi L(1-\rho^2)} \prod_{q=1}^{\infty} (\det \boldsymbol{A}_q)^{1/2} \tag{7}$$

with the kernel matrix diagonal both in q-space and in the d-dimensional coordinate space:

$$\boldsymbol{A}_q = \left[\frac{l_p L}{2}\left(\frac{q\pi}{L}\right)^4 - \mathrm{i}\phi L\left(\frac{q\pi}{L}\right)^2\right]\mathbf{1}_d \qquad \text{and} \qquad \boldsymbol{\rho} = \boldsymbol{R}/L. \tag{8}$$

It is important to note here that we shall not apply the classical approach used in the literature [16] whereby the infinite product of determinants is rewritten as a sum in the exponent, which is then approximated as an integral. Such an approach is very elegant, but is only valid for an infinitely long chain and therefore is not suitable in the stiff chain limit we wish to address here.

Factoring out the arbitrary constant $\prod_{q=1}^{\infty} \frac{1}{2} l_p L^3 (q\pi/L)^4$ out of the determinant and applying the standard identity $\prod_{q=1}^{\infty}[1 - x^2/q^2\pi^2]^{-1} = (x/\sin x)$, we can write the final form of the partition function as

$$Z = \frac{l_p}{2L}\int_{-\infty}^{\infty} \mathrm{d}\xi\, \mathrm{e}^{-\mathrm{i}\xi \frac{l_p}{2L}(1-\rho^2)} \left(\frac{\sqrt{\mathrm{i}\xi}}{\sin\sqrt{\mathrm{i}\xi}}\right)^{d/2}, \tag{9}$$

where in this last step we have used a notation $\xi = 2\phi L^2/l_p$ to bring it to the simple form shown. No approximations are made in the mean-field problem so far.

In order to compare our theory with measured force–extension relations, e.g. [7], it is necessary to find the statistics for chains under the constant tension regime. In this regime the free energy is

$$Z = \int \mathrm{d}\phi\, \mathcal{D}r(s) \exp\left[\int_0^L \mathrm{d}s \left(-\frac{l_p}{2}\ddot{\boldsymbol{r}}(s)^2 + i\phi(\dot{\boldsymbol{r}}(s)^2 - 1) + \beta \boldsymbol{f}\cdot\dot{\boldsymbol{r}}(s)\right)\right] \tag{10}$$

where $\boldsymbol{f}$ is the tension force applied at the chain ends. Applying the boundary conditions and transforming to the same Fourier representation for the arc length, we obtain

$$Z = \frac{l_p}{2L}\int_{-\infty}^{\infty} \mathrm{d}\xi \left(\frac{\sqrt{\mathrm{i}\xi}}{\sin\sqrt{\mathrm{i}\xi}}\right)^{d/2} \exp\left(-\mathrm{i}\xi\frac{l_p}{2L}(1-\rho^2) + \beta \boldsymbol{f}\cdot\boldsymbol{R}\right). \tag{11}$$

As expected, the only effect the external force has on the partition function is to introduce an additional factor of $\exp(\beta \boldsymbol{f}\cdot\boldsymbol{R})$, which is independent of the integration variable ξ. This is a simple Legendre transformation of the resulting free energy.

3. Evaluating the partition function

3.1. Chain confined in two dimensions

For the case $d = 2$, the expression for the partition function in (9) becomes

$$Z_{2\mathrm{D}} \propto \frac{l_p}{2L}\int_{-\infty}^{\infty} \mathrm{d}\xi\, \mathrm{e}^{-\mathrm{i}\xi\gamma} \left(\frac{\sqrt{\mathrm{i}\xi}}{\sin\sqrt{\mathrm{i}\xi}}\right) \tag{12}$$

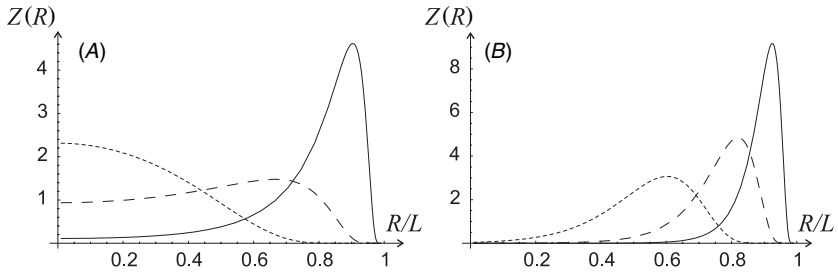

Figure 1. Plots of normalized $Z_{2D}(\rho)$, in the constant-extension (A) and in the constant-force (B) regimes, for the values $L/l_p = 10$ (dotted lines), $L/l_p = 3$ (dashed), $L/l_p = 1$ (solid). In (A) we see that the model correctly approaches the Gaussian distribution for flexible chains, $l_p/L \ll 1$. In (B), where $\beta f = 10/L$ is used, we note that the action of a constant force on the chain increases the most probable value of end-to-end separation, and suppresses the $R \to 0$ states.

where we have introduced the shorthand notation $\gamma = (l_p/2L)(1 - \rho^2)$. As a result, the statistical sum (12) is a non-dimensional integral depending on a single parameter, γ. This expression can be evaluated with no approximation by using complex integration. The integrand possesses simple poles for $i\xi = n^2\pi^2$ with the corresponding residues $2\xi\, e^{-i\xi\gamma} \cos\sqrt{i\xi}$. Choosing a contour that closes in the upper imaginary half-plane, and using the Residue theorem, we find

$$Z_{2D} = \sum_{\xi_j} 2\pi i \times 2\xi_j\, e^{-i\xi_j\gamma} \cos\sqrt{i\xi_j} = \sum_{n=1}^{\infty} (-1)^{n+1} n^2\, e^{-n^2\pi^2\gamma}, \tag{13}$$

where once again we have neglected any arbitrary constant prefactors. Given that we have the statistical weight at a fixed $\rho = R/L$, $Z_{2D}(\rho)$, the corresponding probability distribution $G(R)$ is obtained simply by normalizing $Z_{2D}(\rho)$. A plot of this function for various values of L/l_p is shown in figure 1(A). Note that the maximum in $G(R)$, which corresponds to the statistically most likely state of the semiflexible filament in 2D, occurs for a value of γ which satisfies the following condition:

$$\sum_{n=1}^{\infty} (-1)^n n^4\, e^{-n^2\pi^2\gamma_c} = 0. \tag{14}$$

This is solved numerically and we find $\gamma_c = (l_p/2L)(1 - \rho^2) = 0.0918$ or, equivalently, $(R/L)_c = \sqrt{1 - 0.1836 L/l_p}$.

The extension of this analysis to the constant tension regime is trivial as we simply need to include the additional factor $\exp(\beta f R)$:

$$Z_{2D} = \sum_{n=1}^{\infty} (-1)^{n+1} n^2\, e^{-n^2\pi^2\gamma + \beta f R}. \tag{15}$$

Plots of $Z_{2D}(\rho)$ for a chain under constant tension of $f = 10/\beta L$ is shown in figure 1(B). Qualitatively, applying a constant force to the chain ends shifts the distribution of end-to-end lengths to higher values, which is intuitively what one expects.

3.2. Chain in three dimensions

For the case of $d = 3$, we find the expression in equation (9) difficult to integrate exactly because of the fractional order of singularity. We can, however, perform the

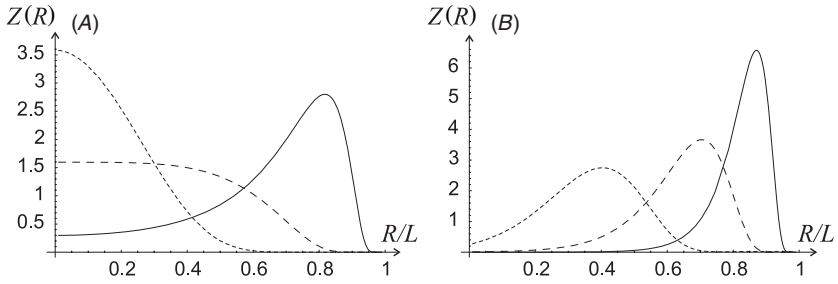

Figure 2. Plots of normalized $Z_{3D}(\rho)$ obtained by numerical integration, in the constant-extension (A) and in the constant-force (B) regimes, for the values $L/l_p = 10$ (narrow dashed lines), $L/l_p = 3$ (wide dashed), $L/l_p = 1$ (solid). We have again used $\beta f = 10/L$. Note the topological similarity between the plots for $d = 2$ and $d = 3$ showing the two cases exhibit the same physical effects.

integration numerically in *Mathematica*, obtaining a universal function of single parameter $\gamma = (l_p/2L)(1 - \rho^2)$. The result of the this integration is a function that is topologically identical to the case for $d = 2$, the only significant difference being that the maximum of $Z_{3D}(\gamma)$ occurs at a larger value, namely $\gamma_c = 0.167$, or $(R/L)_c = \sqrt{1 - 0.332L/l_p}$. The fact that the topology of $Z_{3D}(\rho)$ is the same as $Z_{2D}(\rho)$ means both the $d = 2$ and $d = 3$ cases show the same physical effects; however, the onset of these effects occurs at a different value of γ. The expression for the partition function in the case of constant tension follows again by simply including the additional factor $\exp(\beta f R)$. The functions $Z_{3D}(\rho)$ are plotted in figure 2 for the constant extension regime (A) and constant force regime (B).

Although we could not obtain the exact result for the partition function integral Z_{3D}, it may be useful to offer a tractable analytical interpolation of this non-dimensional function of parameter γ, which contains the universal dependence on R/L and l_p/L. To get an idea of the function we need to use, it is beneficial to look at the approximation to Z_{3D} obtained by the traditional replacing the product $\prod_{q=1}^{\infty}(\det \boldsymbol{A}_q)^{1/2}$ in equation (7) by the integral in the exponent [2, 3, 5]. The details of this approximation, and comparison with other models using it, are given in greater detail in the appendices. Here we just quote equation (B.5) which is valid when $\gamma \ll 1$, and re-write it in terms of this variable only (again, dropping a constant prefactor):

$$Z_{3D} \approx \left[\frac{1}{\gamma^{5/2}} + \frac{9}{4\gamma^{7/2}} + \frac{27}{64\gamma^{9/2}}\right] \mathrm{e}^{-9/16\gamma}. \tag{16}$$

Figure 3(A) shows the numerical result and its comparison with approximated formulae (16) and its leading term, equation (B.6), which is the key result of Ha and Thirumalai [3]. Clearly, a correction that becomes relevant at $\gamma \to 1$ is required for good interpolation, and we decide on the expression that preserves the key features of analytical limiting cases at both $\gamma \ll 1$ and $\gamma \geqslant 1$:

$$Z_{3D} = \left[\frac{2593}{\gamma^{1/2}} + \frac{1627}{\gamma^{3/2}} + \frac{1}{\gamma^{5/2}} + \frac{9}{4\gamma^{7/2}} + \frac{27}{64\gamma^{9/2}}\right] \mathrm{e}^{-9/16\gamma - 9\gamma}. \tag{17}$$

Examining figures 3(A) and (B) one cannot distinguish a difference between the above analytical interpolation and the exact numerical result.

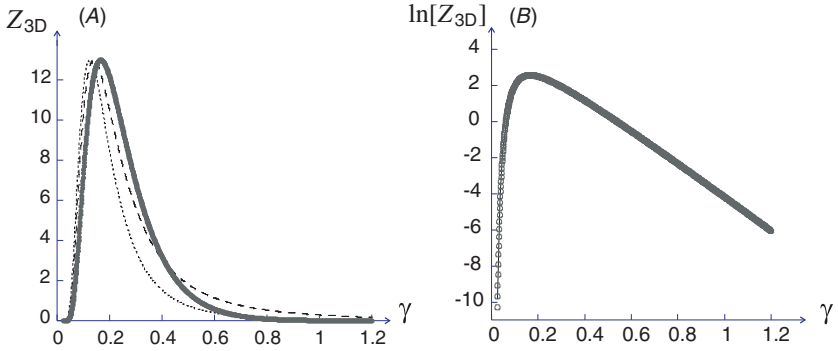

Figure 3. Plots of $Z_{3D}(\gamma)$ comparing the numerical integration of equation (9), shown by grey symbols ○, with its approximations: (*A*) linear plot scale, the leading $\gamma \ll 1$ limit of equation (B.6), dotted line, and the three terms of equations (16) and (B.5), dashed line. The interpolation formula (17), solid line, follows the numerical plot almost exactly. In (*B*), on the logarithmic scale, the interpolation formula (17) can only just be discerned behind the numerical data.

3.3. Radial distribution function $P(\rho)$

It will be useful in comparing our model to experimental data, to define the radial distribution of end-to-end distances $P(\rho)$, which is the normalized probability distribution that $|\boldsymbol{r}(L) - \boldsymbol{r}(0)| = |\boldsymbol{R}|$ irrespective of orientation. The expression for $P(\rho)$ is obtained in the usual way be multiplying the value of the partition function with $\boldsymbol{r}(L) - \boldsymbol{r}(0) = \boldsymbol{R}$ by the spherically symmetric volume element for the required dimension and normalizing.

The resulting radial distribution function takes the form, in 3D and 2D, respectively:

$$P(\rho)_{3D} = \frac{4\pi\rho^2}{\mathcal{N}_3} \times Z_{3D}(\rho), \qquad P(\rho)_{2D} = \frac{2\pi\rho}{\mathcal{N}_2} \times Z_{2D}(\rho) \tag{18}$$

where $\mathcal{N}_i$ are corresponding normalizing constants.

Finally, in many experimental situations microscopic techniques examine chains and filaments deposited on a flat substrate from a 3D solution. In this case, the projection of a 3D distribution onto a plane has to be considered, as shown schematically in figure 4. The projected radial distribution function is obtained by identifying an infinitesimal ring of the radius $R_\perp$ and counting all chains with ends in the volume element $2\pi R_\perp \mathrm{d}R_\perp \mathrm{d}z$ and then sum over all possible z between the limits of maximal and minimal z shown in the diagram, which correspond to the fully stretched chain that projects into $R_\perp$. The resulting projected radial distribution function is then obtained from the partition function, equation (17), by substituting $R \to \sqrt{R_\perp^2 + z^2}$ in its variable γ and integrating

$$P(R_\perp) = \frac{2\pi R_\perp}{\mathcal{N}} \times \int_{z_-}^{z_+} \mathrm{d}z \; Z_{3D}\left(\sqrt{R_\perp^2 + z^2}\right) \tag{19}$$

where $\mathcal{N}$ is the normalization.

4. Results and discussion

In equation (13), we have an expression for the partition function $Z_{2D}(\rho)$ for $d = 2$ that is valid for all stiffnesses. We also have an integral expression, and a full interpolated formula for the partition function $Z_{3D}(\rho)$ for $d = 3$ also valid for all stiffnesses, or chain lengths,

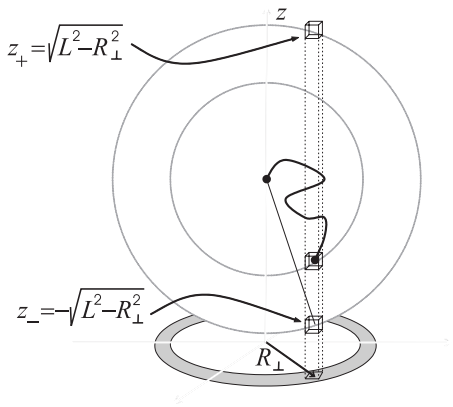

Figure 4. Sketch illustrating the projection of a free 3D chain onto a plane.

equation (17). We would now like to check the physical consequences of these expressions by comparing them with experimental data.

4.1. Force–extension curves

Let us first examine the force–extension curves predicted by this mean-field approach and compare with the results for single DNA molecules [7]. In order to compare our predictions to the data of Smith *et al* [7] it is vital to remember that the experimental results for these force–extension relations were performed in the constant-force regime for the case $d = 3$. That is, Smith *et al* applied a constant tension via magnetic beads to a single DNA strand with $L/l_p \gg 1$ and then measured the *mean* end-to-end separation. It is important to remark that it is the mean, and not the mode that was used i.e. the positions of the ends of the chain were calculated as time averages over the Brownian motion [7]. This subtlety seems to have been overlooked in the majority of the literature. The force–extension relation then follows from expressing the mean $\rho = R/L$ as a function of the applied force f:

$$\overline{\rho} = \int_0^1 \mathrm{d}\rho\, \rho P_{3\mathrm{D}}(\rho, f) = \frac{\int_0^1 \mathrm{d}\rho\, \rho^3 (1-\rho^2)^{-9/2} \exp\left(-\frac{9L}{8l_p(1-\rho^2)} + \beta f L \rho\right)}{\int_0^1 \mathrm{d}\rho\, \rho^2 (1-\rho^2)^{-9/2} \exp\left(-\frac{9L}{8l_p(1-\rho^2)} + \beta f L \rho\right)}. \tag{20}$$

Here we use a limiting form of $Z_{3\mathrm{D}}$ in the $\gamma \ll 1$ limit, given by equation (B.6), which is in effect the Ha–Thirumalai expression, as this is the case in experiments [7] with $L/l_p \gg 1$. Strictly, we could use a more exact form of equation (17), but there is no significant improvement for the data of Smith *et al*. This defines the functional dependence of $\overline{\rho} = h(\beta f L)$ with no free parameters except the ratio L/l_p. This functional dependence is plotted against the results of [7] in figure 5 for the values $T = 37\,^\circ\mathrm{C}$ and $L = 32.7\ \mu\mathrm{m}$ for DNA molecules in 10 mM Na^+ as reported by Smith *et al*.

This close fit is obtained for a value of $L/l_p = 654$. Clearly in this range of pretty flexible chains the use of only the leading term in $Z_{3\mathrm{D}}$ is justified. Given that the measured contour length used in the experiment was $L \sim 32.7\ \mu\mathrm{m}$, both of the fits shown are for a persistence length of $l_p = 50$ nm which is exactly the value of the persistence length reported for the strand of DNA in [7] for the data set used in the fit. Note that the interpolation formula of Marko and Siggia [17] provides a better model at smaller extensions (in the flexible regime). This is unsurprising since our consistent theory uses the mean-field approximation, which works worse at lower extensions (see [6]).

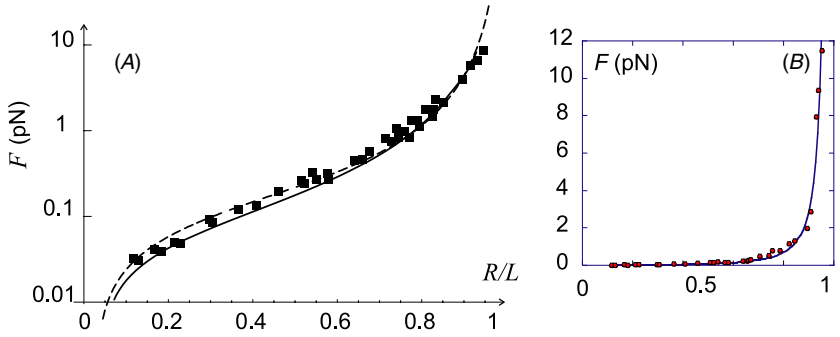

Figure 5. A comparison of the data from experimental force–extension relations on DNA molecules [7] with equation (20). The inset (*B*) shows the data on its natural scale, while the logarithmic plot (*A*) allows much closer comparison with the model. In (*A*) the solid line shows our model fit using the ratio $L/l_p = 654$, which corresponds exactly to the reported $l_p = 50$ nm for the data set used by Smith *et al* i.e. for the DNA strand with contour length 32.7 μm in a 10 mM Na^+ solution. We compare this with the popular interpolation formula of Marko and Siggia (dashed line) [17] which is fitted using the same parameter values.

(This figure is in colour only in the electronic version)

It is important to note that the model will not be applicable for very strong forces. There are three principle reasons for this. Firstly, large tensile forces mean the chain will enter the region $\rho \to 1$ and the inextensibility approximation will begin to break down. That is, at large extensions there will be a non-trivial contribution to the Hamiltonian from energy associated with stretching bonds (see [17]). As shown in [17] this limit occurs only for very large extensions $\rho \approx 0.97$ for the DNA chains used by Smith *et al* [7]. Secondly, it has been shown [18–21] that for large forces the limit of the continuous worm-like chain model and the discrete Kratky–Porod chain are different. For large forces, the limiting behaviour of the discrete chain is in fact that of the freely jointed chain model. The crossover point for the DNA filaments used by Smith *et al* as calculated in [19] would be for forces of order 10 pN. That is, for extensions with $\rho > 0.95$ one would expect the continuum worm-like chain model to become invalid. It should also be noted that in practice, for forces below both of the above regimes, an overstretching transition would occur [22, 23].

4.2. Critical stiffness

The partition functions $Z_{2D}(\rho)$ and $Z_{3D}(\rho)$ develop a pronounced maximum reflecting an extended chain conformation, when the stiffness parameter increases above some critical value. This non-monotonic form of $Z(\rho)$ must not be mixed with the probability distribution $P(\rho)$, which always has a peak at a certain value of $\overline{R}$. The emergence of maximum in $Z(\rho)$, i.e. the minimum of the entropic free energy at a nonzero end-to-end separation, can be understood by examining both equation (9) and its implementations in 2D and 3D. These are universal functions of the parameter γ, with maxima at

$$\gamma_c = 0.0918 \quad (d = 2) \qquad \text{and} \qquad \gamma_c = 0.167 \quad (d = 3). \tag{21}$$

The physical interpretation of this is that as the chain or the filament gets stiffer, the ratio l_p/L increases such that, above the critical value $l_p/L = 2\gamma_c$, there emerges a value of end-to-end separation $\rho = (R/L) \leqslant 1$ that gives a zero force. At even higher l_p/L the value of the preferred relative extension is, therefore, $\rho_c = \sqrt{1 - 2\gamma_c L/l_p}$. For chains and filaments in

this stiff regime, the force on the chain ends for $\rho < \rho_c$ becomes positive, i.e. the filament is 'pushing out' against the force trying to bring the separation of the chain ends to below ρ_c. Mean-field theory therefore predicts that in $d = 3$ the critical value of the ratio L/l_p is approximately 3.0, while in $d = 2$ it is approximately 5.4. These values are in good agreement with the values of 3.85 and 4.5 obtained using a numerical Monte Carlo simulation [4]. For more flexible chains, $l_p/L < 2\gamma_c$, the chain entropy is maximized only when the chain ends are at the same position.

4.3. End-to-end distributions of stiff chains

In the semi-flexible limit, the distribution of end-to-end distances for a given contour length lies somewhere between that wide distribution obtained for flexible (Gaussian) chains, and the delta-function obtained for rod-like chains. Recent experiments [8, 24] have reported the end-to-end distributions for DNA chains and amyloid filaments in this semi-flexible limit. In these experiments, the chains were absorbed on a substrate and visualized by AFM. The precise dynamics of this absorption process is not well understood and so it is unclear whether the absorbed chains on the substrate correspond to chains in $d = 2$, a mathematical projection of $d = 3$ onto $d = 2$, or even that the chains conserve the $d = 3$ distribution on absorption by their stiff segments falling on the surface and rotating as rigid objects.

What is clear from the AFM images is that for contour lengths $L \approx l_p$ there is very little tangling or crossing of filaments. Therefore, the absorption of such rigid filaments onto a substrate would be described by a 2D distribution, if there is some freedom of lateral motion of them along the surface. On the other hand, if the original chain was in the $L/l_p \gg 1$ regime, then on deposition it develops a large number of crossings (overlapping) of its segments, see [8]. In this case the overall distribution has to preserve its original 3D nature, while on a small scale (segments shorter than the overlapping mesh) the locally 2D statistics should be applicable.

We therefore fit the distributions for stiff chains on a substrate with the two-dimensional radial distribution function $P_{2D}(\rho)$. The fits to data obtained from both amyloid filaments [24] are shown in figure 6(*A*). For DNA chains, Valle *et al* [8] have confirmed that they collected the statistics on relatively short segments, of $L = 75$ nm. Figure 6(*B*) shows the fit of the 2D distribution to this data set. For completeness, we also include fits to a 3D distribution projected onto $d = 2$, which as is expected for stiff chain segments, fits very poorly (shown by the dashed curves in both diagrams). Note that for figure 6(*A*) the fitted values l_p for all three curves are consistent with each other, all predicting a persistence length close to 250 nm, which also agrees with independent measurements of filament bending modulus [24]. Figure 6(*B*) suggests a persistence length $l_p = 53$ nm, which is relatively close to the value of 44 ± 3 nm estimated in [8] from a crossover interpolation. (The error bounds on the quoted value of the persistence length in [8] are somewhat questionable as the point of crossover is clearly spread over a broad range; perhaps the value obtained from our fit represents a better approximation.) The reader will also note that the peak in the data in diagram (*B*) is much sharper than the 2D model predicts. We do not know the reason for this, though inclined to believe it may lie in understanding more precisely the process of chain absorption onto and immobilization on the substrate.

It is important to note that although the work of Valle *et al* [8] highlights the importance of self-avoidance for long chains absorbed onto a substrate, the data for the distribution functions in [8] was obtained for chain sections of a fixed 75 nm length. Since this contour length is less than twice the measured persistence length we can safely assume that the issue of self-avoidance is not a relevant one in this regime, and so the good fit by our model is not

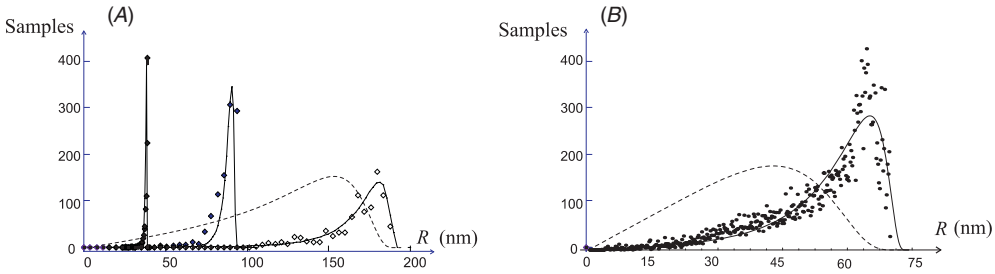

Figure 6. (*A*) Fits of equation (18) to the data of [24]. The data sets correspond to three different contour lengths of the amyloid filaments, $L = 39$ nm, 94 nm and 196 nm, which are then fitted with the free parameter being the persistence length l_p (all three sets give $l_p = 250$ nm). The dashed line shows the fit for $L = 196$ nm and $l_p = 250$ nm assuming a projection from 3D. (*B*) A fit of P_{2D}(solid line) to the data of Valle *et al* [8] for DNA segments of contour length $L = 75$ nm. The fit gives $l_p = 53$ nm. The dashed line shows the 3D-projected distribution function for the value $l_p = 44$ nm quoted in [8].

surprising. Of course, the data of [24] on amyloid filaments are far into the stiff regime, and are therefore fitted very well indeed.

5. Conclusions

Mean-field theory applied to the stiff worm-like chain has the advantage of making the problem analytically tractable. The main advance of this work is the exact analytical treatment of several elements of this problem, which previously required assumptions and approximations.

If we are interested in the statistics of single free chains, the constraint we enforce on the chain must be $\boldsymbol{r}(0) = \boldsymbol{0}$ and $\boldsymbol{r}(L) = \boldsymbol{R}$. In the $\boldsymbol{r}$-space formalism we have used the model of ring with linear shift, equation (6), which serves to constrain the boundary condition and maintains equal forces (measured by $\dot{\boldsymbol{r}}$) on both chain ends. In the alternative formalism, based on the statistics of the tangent vector $\boldsymbol{u}(s)$, one traditionally implements the end-to-end distance constraint by exponentiated delta-function. Appendix A deals with a didactic point of comparison between the two approaches and with earlier approximate models.

Importantly, we conclude that the correct statistics for the free chains of arbitrary stiffness can be obtained by implementing these constraints using only one auxiliary field. That is, we find that the same statistics as Ha and Thirumalai [3] are obtained without the need to introduce separate constraints on the end point tangent vectors $\boldsymbol{u}(0)$ and $\boldsymbol{u}(L)$. However, this conclusion (discussed in appendix B) is only reached when we avoid approximating the Gaussian integrals using the standard technique of exponentiating the determinants, and approximating the sums as integrals. It appears that the need for these additional constraints was linked with the approximations made in calculating the statistical integrals in [3].

In 2D, the partition function integral has been performed exactly using contour integration, while in 3D the integration had to be performed numerically. Nevertheless, the result of this numerical integration is a universal function of a single parameter, which we interpolate nearly exactly by equation (17). Qualitatively (topologically) the properties of the ideal chain are the same in both cases. The model agrees very well with the experimental data of force–extension relations [7] in 3D and equilibrium end-to-end length distributions [8, 24] in 2D. More work, however, needs to be done to fully understand the details of the absorption process in such experiments before careful conclusions can be drawn about the validity of this mean-field model.

Acknowledgments

This work has been supported by the EPSRC TCM/C3 Portfolio. We would like to thank Aidan Craig for many useful discussions, and Giovanni Dietler and Tuomas Knowles for providing their experimental data.

Appendix A. u-space formalism and constraints

The majority of the literature on semi-flexible polymer chains use the tangent vector defined by $\boldsymbol{u}(s) = \partial \boldsymbol{r}/\partial s$ as the variable of the problem [3, 6, 25]. It is certainly reasonable for semi-flexible chains and filaments. We now demonstrate a didactic point, that the $\boldsymbol{u}$-space formulism in mean-field theory [3], where the only conditions on $\boldsymbol{u}$ are that $\langle \boldsymbol{u}^2 \rangle = 1$, is exactly equivalent to the $\boldsymbol{r}$-space formalism developed in section 2.1. In the tangent $\boldsymbol{u}$-space, including the constraints, $\boldsymbol{u}^2 = 1$ for the tangent vector, and the fixed end-to-end separation $\boldsymbol{R}$, we write the partition function as

$$Z = \int \mathcal{D}\boldsymbol{u}(s) \exp\left[-\frac{l_p}{2}\int_0^L \mathrm{d}s \left(\frac{\partial \mathbf{u}}{\partial s}\right)^2\right] \cdot \prod_{s=0}^{s=L} \delta[\boldsymbol{u}(s)^2 - 1] \cdot \delta\left(\boldsymbol{R} - \int_0^L \mathrm{d}s\, \boldsymbol{u}(s)\right). \quad \text{(A.1)}$$

We progress as usual by exponentiating the δ-functions and introducing the auxiliary fields, a scalar $\phi(s)$ and a vector λ, respectively:

$$Z = \int \mathcal{D}\boldsymbol{u}(s) \exp\left[-\frac{l_p}{2}\int_0^L \mathrm{d}s \left(\frac{\partial \boldsymbol{u}}{\partial s}\right)^2\right] \cdot \int \mathcal{D}\phi(s) \exp\left(\mathrm{i}\int_0^L \mathrm{d}s\, \phi(s)[\mathbf{u}(s)^2 - 1]\right)$$
$$\cdot \int L^d\, \mathrm{d}^d\boldsymbol{\lambda} \exp\left(\mathrm{i}\boldsymbol{\lambda} \cdot \left[\mathbf{R} - \int_0^L \mathrm{d}s\, \boldsymbol{u}(s)\right]\right). \quad \text{(A.2)}$$

Here we once again invoke the mean-field approximation for the $\phi(s)$ field. Let us stress that we shall not introduce an additional field to treat the ends of the chain, as in [3] and the subsequent literature.

Since we are dealing with a finite chain length where in general $\boldsymbol{u}(0) \neq \boldsymbol{u}(L)$ we introduce the Fourier series expansion $\boldsymbol{u}(s) = \sum_{q=0}^{\infty} \boldsymbol{u}_q \cos(q\pi s/L)$. Using this representation of $\boldsymbol{u}$ it is clear what the action of the delta-function $\delta\big(\mathbf{R} - \int_0^L \mathrm{d}s\, \boldsymbol{u}(s)\big)$ is. It demands we only sum over configurations for which $\boldsymbol{u}_{q=0} = \boldsymbol{R}/L$ which is exactly the same statement that we use the Fourier series expansion (6) in the $\boldsymbol{r}$-space formalism. Implementing this in the exponents and re-arranging the order of integration in (A.2), we get

$$Z = L^{d+1} \int_{-\infty}^{\infty} \mathrm{d}\phi \int \mathrm{d}^d\lambda \exp(-\mathrm{i}\phi L + \mathrm{i}\boldsymbol{\lambda} \cdot \boldsymbol{R})$$
$$\cdot \int \mathcal{D}\boldsymbol{u}_q \exp\left(-\frac{1}{2}\sum_{q=0}^{\infty} \boldsymbol{u}_q \cdot \mathbf{B}_q \cdot \boldsymbol{u}_q - \mathrm{i}\boldsymbol{\lambda} \cdot \boldsymbol{u}_{q=0} L\right) \quad \text{(A.3)}$$

where the $\mathbf{B}$ matrix is defined by

$$\mathbf{B}_q = \left(\frac{l_p L}{2}\left(\frac{q\pi}{L}\right)^2 - \mathrm{i}\phi L\right)\mathbf{1}_d. \quad \text{(A.4)}$$

Evaluation of Gaussian integrals over $\boldsymbol{u}_{q\neq 0}$ in (A.3) is straightforward, while the $\boldsymbol{u}_{q=0}$ integration requires completing the square first. The combined result of all the $\boldsymbol{u}_q$ integrals

leaves us with

$$Z \propto L^{d+1} \int_{-\infty}^{\infty} \mathrm{d}\phi\, \mathrm{e}^{-\mathrm{i}\phi L} \int \mathrm{d}^d\lambda \exp\left(\mathrm{i}\boldsymbol{\lambda}\cdot\boldsymbol{R} - \frac{\mathrm{i}\boldsymbol{\lambda}^2 L}{4\phi}\right) \prod_{q=0}^{\infty} (\det \mathbf{B}_q)^{1/2}$$

$$\propto L \int_{-\infty}^{\infty} \mathrm{d}\phi\, \mathrm{e}^{-\mathrm{i}\phi L(1-\rho^2)} (4\mathrm{i}\phi L)^{d/2} \prod_{q=0}^{\infty} (\det \mathbf{B}_q)^{1/2} \tag{A.5}$$

where in the final step we have completed the square over $\boldsymbol{\lambda}$. Once again, factoring out the arbitrary constant $\frac{1}{2\pi} l_p L \prod_{q=1}^{\infty} (q\pi/L)^2$, the partition function reduces to the form:

$$Z = \frac{l_p}{2L} \int_{-\infty}^{\infty} \mathrm{d}\xi\, \mathrm{e}^{-\mathrm{i}\xi \frac{l_p}{2L}(1-\rho^2)} \left(\frac{\sqrt{\mathrm{i}\xi}}{\sin\sqrt{\mathrm{i}\xi}}\right)^{d/2}, \tag{A.6}$$

with $\xi = 2\phi L^2/l_p$. Noting that this is the exact same expression as that obtained in the $\boldsymbol{r}(s)$-formalism, we have thus demonstrated the equivalence between the two representations. This verifies that the constraint $\delta\big(\boldsymbol{R} - \int_0^L \mathrm{d}s\, \boldsymbol{u}(s)\big)$ in the $\boldsymbol{u}$-space approach is equivalent to the use of the 'ring + linear shift' condition in equation (6).

Appendix B. Validating the use of single auxiliary field

In order to validate the use of only one auxiliary field to implement the average constraint $\langle \boldsymbol{u}^2 \rangle = 1$, we now reproduce the results of Ha and Thirumalai by evaluating the partition function in the limit $L \gg l_p$ for the case $d = 3$, without the need for an extra Lagrange multiplier to deal with the ends of the chain [3, 6]. We progress by setting $d = 3$ and re-writing equation (A.5) as

$$Z = L \int_{-\infty}^{\infty} \mathrm{d}\phi\, \mathrm{e}^{-\mathrm{i}\phi L(1-\rho^2)} (4\mathrm{i}\phi L)^{3/2} \prod_{q=0}^{\infty} \left[1 - \frac{2\mathrm{i}\phi L^2}{l_p q^2 \pi^2}\right]^{-3/2}$$

$$= L \int_{-\infty}^{\infty} \mathrm{d}\phi\, (4\mathrm{i}\phi L)^{3/2} \exp\left(-\mathrm{i}\phi L(1-\rho^2) - \frac{3}{2} \sum_{q=0}^{\infty} \left[1 - \frac{2\mathrm{i}\phi L^2}{l_p q^2 \pi^2}\right]\right).$$

Remaining in the limit $L \gg l_p$ we can approximate the sum as an integral:

$$\sum_{q=0}^{\infty} \ln\left(1 - \frac{2\mathrm{i}\phi L^2}{l_p q^2 \pi^2}\right) \approx \int_0^{\infty} \mathrm{d}q \ln\left(1 - \frac{2\mathrm{i}\phi L^2}{l_p q^2 \pi^2}\right) = \mathrm{i}L\sqrt{\frac{2\mathrm{i}\phi}{l_p}}, \tag{B.1}$$

plus several constant terms, which are neglected as they simply shift the final free energy. The partition function then becomes

$$Z = L \int_{-\infty}^{\infty} \mathrm{d}\phi\, (4\pi\,\mathrm{i}\phi L)^{3/2} \exp\left(-\mathrm{i}\phi L(1-\rho^2) - \frac{3\mathrm{i}L}{2}\sqrt{\frac{2\mathrm{i}\phi}{l_p}}\right). \tag{B.2}$$

The common approach at this stage is to evaluate the integral by steepest descent [2], which will give a result that differs from Ha and Thirumalai. However, we can perform this integration analytically, by making a substitution $\mathrm{i}\phi \to x^2$ and completing the square over x, to obtain

$$Z \propto L^{5/2} \exp\left(-\frac{9L}{8l_p(1-\rho^2)}\right) \int_{-\infty}^{\infty} \mathrm{d}x\, x^4\, \mathrm{e}^{-a(x+b)^2} \tag{B.3}$$

where

$$a = L(1-\rho^2), \qquad b = \frac{3}{\sqrt{8l_p}(1-\rho^2)}. \tag{B.4}$$

The integral is now in standard Gaussian form and can easily be evaluated:

$$Z = \left[\frac{1}{(1-\rho^2)^{5/2}} + \frac{9L}{2l_p(1-\rho^2)^{7/2}} + \frac{27L^2}{16l_p^2(1-\rho^2)^{9/2}} \right] \mathrm{e}^{-\frac{9L}{8l_p(1-\rho^2)}}. \tag{B.5}$$

The approximation in (B.1) is only valid for chains with small stiffness $l_p/L \ll 1$. Retaining only the leading term in this limit, equation (B.5) gives the approximate partition function and the corresponding free energy:

$$Z \approx (1-\rho^2)^{-9/2}\, \mathrm{e}^{-\frac{9L}{8l_p(1-\rho^2)}}, \qquad \beta F \approx \frac{9L}{8l_p(1-\rho^2)} + \frac{9}{2}\ln(1-\rho^2). \tag{B.6}$$

These expressions are exactly the same as those obtained by Ha and Thirumalai [3], but obtained here using only one auxiliary field $\langle \phi(s) \rangle = \phi$ and without the need to introduce additional Lagrangian multipliers to control the (free) ends of the chain.

References

[1] Kratky O and Porod G 1949 *Rec. Trav. Chim.* **68** 1106
[2] Vilgis T A, Otto M and Eckert J 1994 *Macromol. Theory Simul.* **3** 543
[3] Thirumalai D and Ha B Y 1999 *Theoretical and Mathematical Models in Polymer Research* ed A Grosberg (New York: Academic)
[4] Dhar A and Chaudhuri D 2002 *Phys. Rev. Lett.* **89** 065502
[5] Craig A and Terentjev E M 2006 *J. Phys. A: Math. Gen.* **39** 4811
[6] Winkler R G 2003 *J. Chem. Phys.* **118** 2919
[7] Smith S B, Finzi L and Bustamante C 1992 *Science* **258** 1122
[8] Valle F, Favre M, De Los Rios P, Rosa A and Dietler G 2005 *Phys. Rev. Lett.* **97** 158105
[9] Sharp P and Bloomfield V A 1968 *Biopolymers* **6** 1201
[10] des Cloizeaux J 1973 *Macromolecules* **6** 403
[11] Pincus P 1976 *Macromolecules* **9** 386
[12] Toan N M, Marenduzzo D and Micheletti C 2005 *Biophys. J.* **89** 80
[13] Lam Y H 2002 *Biopolymers* **64** 57
[14] Mooney M 1959 *J. Polym. Sci.* **304** 599
[15] Doi M and Edwards S F 1986 *The Theory of Polymer Dynamics* (Oxford: Clarendon)
[16] Edwards S F and Gupta A M 1992 *J. Chem. Phys.* **98** 1588
[17] Marko J F and Siggia E D 1995 *Macromolecules* **28** 8759
[18] Odijk T 1995 *Macromolecules* **28** 7016
[19] Rosa A, Hoang T X, Marenduzzo D and Maritan A 2003 *Macromolecules* **36** 10095
[20] Livadaru L, Netz R R and Kreuzer H J 2003 *Macromolecules* **36** 3732
[21] Kleinert H 2004 *Path Integrals in Quantum Mechanics, Statistics, Polymer Physics and Financial Markets* 3rd edn (Singapore: World Scientific)
[22] Smith S B, Cui Y and Bustamante C 1996 *Science* **271** 795
[23] Storm C and Nelson P C 2003 *Phys. Rev.* E **67** 051906
[24] Knowles T P J, Smith J F, Craig A, Dobson C M and Welland M E 2006 *Phys. Rev. Lett.* **98** 238301
[25] Wilhelm J and Frey E 1996 *Phys. Rev. Lett.* **77** 2581